

Optimal Transportation Methods in Nonlinear Filtering

The feedback particle filter

Amirhossein Taghvaei and Prashant G. Mehta

March 2, 2022

How Data Became One of the Most Powerful Tools to Fight an Epidemic is a question that a recent (Jun 10 2020) NYT magazine article poses in its title and addresses in its content. Indeed, the spread of COVID-19 involves dynamically evolving hidden data (e.g., number of infected, number of asymptomatic etc.) that must be deduced from noisy and partially observed data (e.g., number of daily deaths, number of daily hospitalized, number of daily tested positive etc.). The underlying mathematics for posing and solving this and several other partially observed dynamic problems is familiar to most control theorists.

A mathematical abstraction of these types of problems commonly involves definition of two stochastic processes (X, Z) where in continuous-time settings $X = \{X_t \in \mathbb{S} : t \geq 0\}$ is the hidden signal process and $Z = \{Z_t \in \mathbb{O} : t \geq 0\}$ is the observed or measured process. For the sake of exposition, the state-space \mathbb{S} and the observation-space \mathbb{O} are assumed to be the Euclidean spaces, and the two processes are modeled as solution of a stochastic differential equation (SDE)

$$dX_t = a(X_t) dt + \sigma(X_t) dB_t, \quad X_0 \sim (\text{prior}), \quad (1)$$

$$dZ_t = h(X_t) dt + dW_t, \quad Z_0 = 0, \quad (2)$$

where $a(\cdot), \sigma(\cdot), h(\cdot)$ are given smooth functions of their arguments, the signal (or process) noise $B = \{B_t : t \geq 0\}$ and the measurement (or observation) noise $W = \{W_t : t \geq 0\}$ are assumed to be independent Wiener processes (w.p). For example, in the models of disease spread, Z_t may indicate the number (cumulative) of tested positive up to time t . In this case, $Z_{t_2} - Z_{t_1}$ is the number (increment) of tested positive during the time interval $[t_1, t_2]$, and “ dZ_t ” can be thought of as the infinitesimal increment over the infinitesimal time “ dt ”.

Given models for the stochastic processes (X, Z) , the mathematical problem of stochastic filtering is to estimate the conditional distribution of the state X_t given observations up to time t . The conditional distribution $P(X_t | \mathcal{Z}_t)$ is referred to as the posterior distribution where \mathcal{Z}_t is the time-history (filtration) of observations up to time t .

Owing the widespread importance of this problem, there are a host of solution approaches under different modeling assumptions. The most classical of these approaches is the method of least squares. The method was invented at the turn of the 19th century but remains popular to date, for instance, in identification of the (static) model parameters (see [1] for an application of these methods to parameter estimation in disease modeling). For the dynamic case, when the models are linear (i.e., $a(x) = Ax$, $\sigma(x) = \sigma$ and $h(x) = Hx$) and the distributions (of the noise processes and the prior) are Gaussian, Kalman and Bucy derived a recursive algorithm [2] known as the Kalman-Bucy filter

$$d\hat{X}_t = \underbrace{A\hat{X}_t dt}_{\text{dynamics}} + \underbrace{K_t(dZ_t - H\hat{X}_t dt)}_{\text{control}},$$

where $\hat{X}_t := E(X_t|Z_t)$ is the conditional mean and K_t is the Kalman gain. Each of the two terms on the right-hand side have an intuitive explanation. The first term accounts for the effect of the dynamics due to the signal model. The second term implements the effect of conditioning because of the most recent observation (increment) “ dZ_t ”. The second term is referred to as the correction or the Bayes’ update step of the Kalman filter.

It is remarkable that the Bayes’ update formula in the Kalman filter takes the form of a feedback control law where

$$[\text{control}] = [\text{gain}] \cdot [\text{error}],$$

and

$$[\text{error}] = [\text{Observation}] - [\text{prediction}].$$

Note that “ $H\hat{X}_t dt$ ” is the filter prediction of the new observation “ dZ_t ”. The formula is so simple that it can and should be part of any introductory undergraduate controls class – as an example of proportional gain feedback control law! Of course, this simple formula has had an enormous impact in many applications such as target tracking and surveillance, air traffic management, weather surveillance, ground mapping, geophysical surveys, remote sensing, autonomous navigation and robotics.

The Kalman filter has many extensions, for example, to problems involving additional uncertainties in the signal and the observation models. The resulting algorithms are referred to as the interacting multiple model (IMM) filter [3] and the probabilistic data association (PDA) filter [4], respectively. In the PDA filter, the Kalman gain is allowed to vary based on an estimate of the instantaneous uncertainty in the observations. In the IMM filter, multiple Kalman filters are run in parallel and their outputs combined to form an estimate.

Arguably, the structural aspects of the Kalman filter have been as important as the algorithm itself in design, integration, testing and operation of the overall system. As a simple illustration

of this, consider for example the Kalman filter gain. The gain is known to scale proportionally to the signal-to-noise ratio (SNR) of the observations. In practice, the gain is often tuned or adapted in an online manner to trade-off performance for robustness. Without such structural features, it is a challenge to create scalable cost-effective robust solutions.

A limitation of the Kalman filter is that it gives exact solution only in the linear Gaussian settings. Beginning in early 1990s, spurred in part by computational advances, simulation-based Monte-Carlo (MC) algorithms became popular for the purposes of numerically approximating the posterior distribution in more general settings. These class of algorithms, referred to as particle filters, approximate the posterior distribution using a population of N particles $\{X_t^i : t \geq 0, 1 \leq i \leq N\}$. One can interpret each of the particles as independent samples drawn from the posterior. Alternatively, one can interpret the empirical distribution of the population as approximating the posterior distribution.

Like the Kalman filter, the particle filter too is a recursive algorithm. The signal model is used to simulate the effect of the dynamics. The Bayesian update step is implemented using techniques such as importance sampling and resampling. Although these techniques are easily described, they bear little resemblance to the feedback control structure of the Kalman filter.

The focus of the present paper is on the feedback particle filter (FPF) algorithm. FPF represents an exact solution of the nonlinear non-Gaussian filtering problem (1)-(2) where the state-space \mathbb{S} can in general be a Riemannian manifold. (In applications, Euclidean spaces and matrix Lie groups are most common.) The distinguishing feature of the FPF is that the Bayesian update step is implemented via a feedback control law of the form

$$[\text{control}] = [\text{gain}] \cdot [\text{error}],$$

where

$$[\text{error}] = [\text{Observation}] - \left(\frac{1}{2} [\text{Part. predict.}] + \frac{1}{2} [\text{Pop. predict.}] \right).$$

The terms [Part. predict.] and [Pop. predict.] refer to the prediction – regarding the next [Observation] “ dZ_t ” – as made by the particle and by the population, respectively (see the diagram 1). Because the control for each particle depends also on the population (and thus the empirical distribution), this is an example of a mean-field type control law; cf., [5], [6]. It turns out that for the linear Gaussian problem in the Euclidean state-space, the [gain] of the FPF is exactly the Kalman gain. In non-Gaussian settings, the gain solves a certain linear partial differential equation (PDE) known as the weighted Poisson equation. The exact formula for the FPF control and gain appears in the main body of the paper.

At the turn of the decade beginning 2010, the FPF algorithm was introduced by our research group at the University of Illinois [7], [8], [9]. The algorithm can be viewed as a modern extension to the Kalman filter, a viewpoint stressed in a prior review paper [10]. Like the Kalman filter, the FPF is easily extended to handle additional uncertainties in signal and measurement model: These extensions, namely, the joint probabilistic data association (JPDA)-FPF and the interacting multiple model (IMM) FPF appear in our prior works [11], [12].

From a historical perspective, FPF is part of a broader class of exact and approximate interacting particle algorithms, in particular, the ensemble Kalman filter (EnKF) which is widely used for data assimilation in weather prediction and other types of geo-physical applications [13]. Closely related to and pre-dating our work on FPF, the first interacting particle representation of the continuous-time nonlinear filtering problem (1)-(2) appeared in [14]. In linear Gaussian settings, the update formula for FPF is known as the square root form of the EnKF [15], [16].

The objective for this paper is to situate the development of FPF and related controlled interacting particle system algorithms (e.g., EnKF) within the framework of optimal transportation theory. The key notion is that of “coupling” between two distributions – prior and posterior in the Bayesian settings of this paper. Optimal transportation theory is then applied to design the optimal coupling. Of course, in practice, this requires a solution of certain PDEs – such as the Poisson equation that arise in the FPF algorithm. The coupling viewpoint has several advantages which are described in the main body of this paper.

The coupling viewpoint

The heart of any simulation-based recursive particle filter algorithm is the Bayes’ update formula

$$[\text{posterior}] \propto [\text{likelihood}] \cdot [\text{prior}].$$

The notation $p_0(\cdot)$, $p_1(\cdot)$, and $\ell(\cdot)$ is used to denote the prior, posterior, and likelihood distributions respectively. The expressions for these in the linear Gaussian example appear in “optimal coupling for Gaussian distributions”.

In any particle filter algorithm, one also needs to simulate the effect of dynamics. This step is straightforward using the signal model directly. Therefore, we focus here only on the update formula.

In simulation settings, one of the challenges is that an analytic expression of the prior distribution is not available. Instead, the prior is approximated in terms of N independent samples

$\{X_0^i : 1 \leq i \leq N\}$:

$$p_0(x) \approx \frac{1}{N} \sum_{i=1}^N \delta_{X_0^i}(x),$$

where δ_z is the Dirac distribution at $z \in \mathbb{S}$. The expression on the right-hand side is referred to as the empirical distribution of the population. Alternatively, one can think of X_0^i as independent samples drawn from the prior.

In a numerical implementation of the update formula, the problem is to convert the sample of N particles $\{X_0^i : 1 \leq i \leq N\}$ from the prior distribution $p_0(\cdot)$ to a sample of N particles $\{X_1^i : 1 \leq i \leq N\}$ from the posterior distribution $p_1(\cdot)$. The algorithmic problem is depicted in Figure 2 and expressed as follows

Input: samples $\{X_0^i : 1 \leq i \leq N\} \sim p_0$, likelihood function ℓ ,
Output: samples $\{X_1^i : 1 \leq i \leq N\} \sim p_1$.

The task of converting samples from one distribution $p_0(\cdot)$ to samples from another distribution $p_1(\cdot)$ is viewed here as the problem of finding a coupling $\pi(\cdot, \cdot)$; cf., [17], [18], [19]. By definition, a coupling is any joint probability distribution that satisfies the marginal constraints $\int \pi(x, x') dx' = p_1(x)$ and $\int \pi(x, x') dx = p_0(x')$. It is convenient to express $\pi(x, x') = \mathcal{T}(x|x') p_0(x')$ where $\mathcal{T}(\cdot|\cdot)$ is referred to as the transition kernel. Once the coupling is at hand, new samples are generated by using the transition kernel.

Given this viewpoint, the MC algorithm simulates the following stochastic update law for the system of particles:

$$X_1^i \sim \mathcal{T}(\cdot|X_0^i). \quad (3)$$

This means that a new sample X_1^i is generated by sampling from the distribution $\mathcal{T}(\cdot|X_0^i)$. The sampling algorithm (3) ensures that if the probability distribution of X_0^i is p_0 then the probability distribution of X_1^i is p_1 . The associated algorithmic task is expressed as

Input: samples $\{X_0^i : 1 \leq i \leq N\} \sim p_0$, likelihood function ℓ ,
Output: coupling between p_0 and p_1 .

SIR particle filter

There are infinitely many couplings between two distributions. The simplest possible choice is an independent coupling where $\pi(x, x') = p_1(x)p_0(x')$. For the independent coupling, the transition kernel $\mathcal{T}(x|x') = p_1(x)$. Sequential importance resampling (SIR) particle filters [20], [21] numerically implement the independent coupling in two steps:

Step 1: A weighted distribution of the particles is first formed according to $\sum_{i=1}^N w_i \delta_{X_0^i}$ where the weights $w_i = \frac{l(X_0^i)}{\sum_{j=1}^N l(X_0^j)}$. The weighted distribution is an approximation of the posterior distribution p_1 . This step is called importance sampling.

Step 2: Next N particles are independently sampled from the weighted distribution: $X_1^i \sim \sum_{i=1}^N w_i \delta_{X_0^i}$, by sampling from a multinomial distribution with parameter vector $(N, \{w_i\}_{i=1}^N)$. This step is called resampling.

Theoretically, it is shown that the empirical approximation with particles becomes exact in the limit as $N \rightarrow \infty$ with error rate $O(N^{-1/2})$ [22], [23]. However, both empirically and theoretically, it was discovered that particle filters can suffer from large simulation variance that progressively gets worse as the dimension of the problem increases [24], [25], [26]. To maintain the same mean-squared error, a particle filter is known to require a number of particles that scales exponentially with the dimension. This issue is referred to as the *curse of dimensionality* (CoD).

The issues with the stochastic independent coupling in SIR filters has motivated investigation of other forms of coupling that are also optimal in some sense [27], [28]. In the simulation literature, this is referred to as the design of proposal distributions.

Optimal transport coupling

Optimal transportation theory provides a principled approach to identify a coupling. Given two distributions p_0 and p_1 , the optimal transportation problem is

$$\min_{\pi \in \Pi_{p_0, p_1}} \mathbb{E}_{(X_0, X_1) \sim \pi} [|X_0 - X_1|^2], \quad (4)$$

where Π_{p_0, p_1} is the set of all couplings with marginals fixed to p_0 and p_1 . The optimal cost is referred to as L^2 -Wasserstein distance between p_0 and p_1 [29].

The optimization problem (4) is known as the Kantorovich formulation of the optimal transportation problem. By a famous result due to Brenier, if the two distributions admit density with respect to Lebesgue measure, then the optimal coupling is unique and deterministic of the form $\pi(x, x') = \delta_{x=\nabla\Phi(x')} p_0(x')$ where Φ is a convex function [29, Thm. 2.12]. The function Φ is obtained by solving the Monge-Ampère PDE [30]. A numerical solution to the Monge-Ampère PDE based only on the samples is a challenging problem. In the following, we discuss the special setting where the prior and posterior distributions are Gaussian.

Optimal coupling for Gaussian distributions

In Gaussian settings, the prior and the likelihood are both Gaussian distributions:

$$p_0(x) \propto \exp\left(-\frac{1}{2}(x - m_0)^\top \Sigma_0^{-1}(x - m_0)\right), \quad l(x) \propto \exp\left(-\frac{|y - Hx|^2}{2}\right).$$

In this case, a simple completion of square helps show that the posterior is also a Gaussian distribution

$$p_1(x) \propto \exp\left(-\frac{1}{2}(x - m_1)^\top \Sigma_1^{-1}(x - m_1)\right).$$

This yields the following update formula for the mean and variance:

$$m_1 = m_0 + K(Y - Hm_0), \quad \Sigma_1 = \Sigma_0 - KH\Sigma_0,$$

where $K = \Sigma_0 H^\top (H\Sigma_0 H^\top + I)^{-1}$ is the Kalman gain. This is in fact the update formula for the discrete-time Kalman filter.

The coupling design problem is to couple the Gaussian prior p_0 and the Gaussian posterior p_1 . The optimal coupling, solution to the optimal transportation problem (4), between two Gaussian distributions is explicitly known and is an affine map of the form

$$T(x) = F(x - m_0) + m_1, \tag{5}$$

where F is the (unique such) symmetric matrix solution to the matrix equation $F\Sigma_0 F = \Sigma_1$. The explicit form of the solution is

$$F = \Sigma_0^{-\frac{1}{2}} \left(\Sigma_0^{\frac{1}{2}} \Sigma_1 \Sigma_0^{\frac{1}{2}} \right)^{\frac{1}{2}} \Sigma_0^{-\frac{1}{2}}.$$

Note that if $X \sim \mathcal{N}(m_0, \Sigma_0)$ then $T(X) \sim \mathcal{N}(m_1, \Sigma_1)$ because: (i) the mean $\mathbb{E}[T(X)] = m_{k+1}$; (ii) the variance $\mathbb{E}[(T(X) - m_1)(T(X) - m_1)^\top] = F\Sigma_0 F = \Sigma_1$; (iii) and an affine transformation of a Gaussian random variable is again Gaussian.

The optimal transport map (5) yields the following algorithm for sampling

$$X_1^i = T(X_0^i) = F(X_0^i - m_0) + m_1.$$

Given $X_0^i \sim p_0$ we have $X_1^i \sim p_1$.

The optimal coupling depends upon the statistics of both the prior and the posterior distributions. In simulation-based setting, one only has a population of particles $\{X_0^i : 1 \leq i \leq N\}$. So, the transport map needs also to be approximated from the particles. One such approximation is as follows:

$$\text{particle update: } X_1^i = F^{(N)}(X_0^i - m_0^{(N)}) + m_0^{(N)} + K^{(N)}(Y - Hm_0^{(N)}), \tag{6}$$

where $m_0^{(N)} = \frac{1}{N} \sum_{i=1}^N X_0^i$ is an empirical approximation of the mean m_0 , $\Sigma_0^{(N)} = \frac{1}{N-1} \sum_{i=1}^N (X_0^i - m_0^{(N)})(X_0^i - m_0^{(N)})^\top$ is an empirical approximation of the variance, $F^{(N)}$ is the unique symmetric matrix solution to the matrix equation $F^{(N)} \Sigma_0^{(N)} F^{(N)} = \Sigma_0^{(N)} - K^{(N)} H \Sigma_0^{(N)}$, and $K^{(N)} = \Sigma_0^{(N)} H^\top (H \Sigma_0^{(N)} H^\top + I)^{-1}$.

The update formula (6) is compared to the discrete-time EnKF update:

$$\text{particle update (EnKF): } X_1^i = X_0^i + K^{(N)}(Y - H X_0^i + W^i), \quad (7)$$

where $\{W^i : 1 \leq i \leq N\}$ are independent copies of the observation noise. The EnKF update is an example of a stochastic coupling in contrast to the deterministic optimal coupling (6). The EnKF update does not require solving for $F^{(N)}$. This makes it simpler to implement numerically. However, the presence of noise W^i in the update law introduces an additional source of error in any finite- N implementation [31].

Besides (7), there are several other forms of the EnKF update. One particular update – that has been crucial in successful application of EnKF in geosciences – is the ensemble square-root Kalman filter (EnSRKF) [32]. This update is an example of a deterministic coupling that also avoids the need to compute $F^{(N)}$ [17, Sec. 7.1]. In the sequel, the continuous-time version of the EnSRKF is shown to arise as a special case of the FPF.

The systems (6) and (7) are both examples of interacting particle system. The interaction arises because of the terms involving the empirical quantities $m_0^{(N)}$ and $\Sigma_0^{(N)}$. In the limit as $N \rightarrow \infty$, these converge to their respective statistics and the particles become independent of each other [33], [34], [35], [36], [37]. This phenomenon is referred to as the propagation of chaos [38], [39]. The $(N = \infty)$ limit is referred to as the mean-field limit and for (6) it is identified with a single equation

$$\text{mean-field update: } \bar{X}_1 = F(\bar{X}_0 - m_0) + m_0 + K(Y - H m_0). \quad (8)$$

As a practical matter, one first designs a coupling (5) which is used to define the mean-field process (8). Subsequently, the mean-field terms are approximated empirically to define a particle system (6). A finite- N implementation of the particle system yields a practical algorithm to solve the filtering task.

A summary of this subsection is presented in the sidebar “Summary of the linear Gaussian example”. An excellent exposition of the coupling approach to discrete-time filtering appears in the monograph [17] and the tutorial style review article [18]. Other examples of couplings include the approximation of the Rosenblatt transport map [40], [41] and Gibbs flow [42].

Feedback particle filter

The coupling viewpoint is next employed to introduce and describe the feedback particle filter (FPF) algorithm. FPF is a MC solution to the continuous-time nonlinear filtering problem (1)-(2).

A construction of FPF proceeds in the following two steps:

Step 1: Construct a stochastic process $\bar{X} = \{\bar{X}_t \in \mathbb{S} : t \geq 0\}$ such that the conditional distribution (given \mathcal{Z}_t) of \bar{X}_t is equal to the posterior distribution of X_t ;

Step 2: Simulate N stochastic processes $\{X_t^i \in \mathbb{S} : t \geq 0, 1 \leq i \leq N\}$ to empirically approximate the conditional distribution of \bar{X}_t .

$$\underbrace{\mathbb{E}[f(X_t)|\mathcal{Z}_t]}_{\text{exactness condition}} \stackrel{\text{Step 1}}{=} \mathbb{E}[f(\bar{X}_t)|\mathcal{Z}_t] \stackrel{\text{Step 2}}{\approx} \frac{1}{N} \sum_{i=1}^N f(X_t^i).$$

for all bounded functions f . The process \bar{X} is referred to as mean-field process and the N processes are referred to as particles. The construction ensures that the filter is *exact* in the mean-field ($N = \infty$) limit.

Mean-field process: The mean-field process \bar{X} is modeled as a solution of a controlled SDE:

$$d\bar{X}_t = \underbrace{a(\bar{X}_t) dt + \sigma(X_t) d\bar{B}_t}_{\text{dynamics}} + \underbrace{u_t(\bar{X}_t) dt + K_t(\bar{X}_t) dZ_t}_{\text{control}}, \quad \bar{X}_0 \stackrel{d}{=} X_0, \quad (9)$$

where $\bar{B} = \{\bar{B}_t : t \geq 0\}$ is a w.p. independent of \bar{X}_0 . The first two terms in the SDE (9) are a copy of the dynamics (1). The other two terms are control laws (transition kernels) that need to be designed to implement the filtering update step: The mathematical control objective is to design $\{u_t(\cdot) : t \geq 0\}$ and $\{K_t(\cdot) : t \geq 0\}$ such that the conditional distribution (given \mathcal{Z}_t) of \bar{X}_t is equal to the posterior distribution of X_t .

The control is regarded as implementing the transition kernel of a coupling. As in the simpler discrete-time setting of the preceding section, there are infinitely many couplings and associated transition kernels that satisfy the exactness criteria. This is not surprising: The exactness condition specifies only the marginal distribution of \bar{X}_t at times $t \geq 0$. This is clearly not enough to uniquely identify a stochastic process, for instance, the joint distributions at two time instants are not specified.

The procedure from the preceding section is suitably adapted to design the optimal coupling. The optimality criterion is the Kantorovich form (4) of the optimal transportation

problem. The details appear in the sidebar “Optimal transport construction of stochastic processes” where it is shown that the optimal K_t is of the gradient form as follows:

$$K_t(x) = \nabla \phi_t(x), \quad \text{where } \phi_t \text{ solves the PDE} \quad -\nabla \cdot (p_t \nabla \phi_t) = p_t(h - \hat{h}_t),$$

where ∇ is the gradient operator, $\nabla \cdot$ is the divergence operator, $\hat{h}_t := \mathbb{E}[h(\bar{X}_t)|\mathcal{Z}_t] = \int h(x)p_t(x)dx$, and p_t is the conditional density of \bar{X}_t .

The optimal solution for u_t is as follows:

$$u_t(x) = -\frac{1}{2}(h(x) + \hat{h}_t)K_t(x) + \frac{1}{2}K_t \nabla K_t(x) + \xi_t(x),$$

where ξ_t is the (unique such) divergence-free vector field (i.e., $\nabla \cdot (p_t \xi_t) = 0$) such that u_t is of a gradient form. An intuitive explanation of the three terms is as follows: The first term is the gain times the average at the ‘particle’ prediction $h(x)$ and the population prediction \hat{h}_t . Together with the stochastic term $K_t dZ_t$, the first term yields the gain times error structure of the FPF. The second term is the so-called Wong-Zakai correction term from which it follows that the gain times error formula is expressed in its Stratanovich form. (The geometric significance of the Stratanovich form is described after the FPF formula has been formally presented.) The significance of the third term is the subject of the next paragraph.

It turns out that the divergence-free choices of ξ_t parametrize a manifold of couplings all of which yield the same (exact) posterior. Therefore, the choice of ξ_t affects *only* the (Wasserstein) optimality but not the exactness property of the filter. In FPF, we simply take $\xi_t \equiv 0$ for all $t \geq 0$. Although such a solution is optimal only in the scalar (one-dimensional) settings, it avoids the need to solve an additional PDE to compute the optimal ξ_t . The resulting algorithm is referred to as the feedback particle filter. It is described next.

Feedback particle filter: The mean-field process \bar{X} evolves according to the SDE:

$$d\bar{X}_t = \underbrace{a(\bar{X}_t)dt + \sigma(X_t)d\bar{B}_t}_{\text{dynamics}} + \underbrace{K_t(\bar{X}_t) \circ \left(dZ_t - \frac{h(\bar{X}_t) + \hat{h}_t}{2} dt \right)}_{\text{Bayes' update: feedback control law}}, \quad \bar{X}_0 \sim p_0, \quad (10)$$

where the symbol \circ is used to denote the fact that the SDE is expressed in its Stratanovich form [43, Sec. 3.3]. The Itô form of the FPF includes the standard Wong-Zakai correction term that arises on account of the dependence of the gain $K_t(\cdot)$ on the state X_t [44, Eq. 2]. Because the gain also depends upon the density, the interpretation of the Stratonovich form in the general case is more involved as discussed at length in [45].

The gain function is $K_t(x) := \nabla \phi_t(x)$ where ϕ_t is the solution of the Poisson equation:

$$\text{Poisson equation:} \quad -\frac{1}{p_t(x)} \nabla \cdot (p_t(x) \nabla \phi_t(x)) = (h(x) - \hat{h}_t), \quad \forall x \in \mathbb{R}^d. \quad (11)$$

The operator on the left-hand side of (11) is the *probability-weighted Laplacian*. It is denoted as $\Delta_\rho := \frac{1}{\rho} \nabla \cdot (\rho \nabla)$ where at time t the probability density ρ is the conditional density p_t . The equation (11) is referred to as the Poisson equation of nonlinear filtering [46].

The Stratanovich form of the update formula provides for an intrinsic (i.e., coordinate independent) description of the filter. It was shown that the FPF is an exact filter not only in the Euclidean settings but also when the state-space \mathbb{S} is a Riemannian manifold, e.g., a matrix Lie group [47]. For a manifold with boundaries, the Poisson equation is supplemented with the Neumann boundary conditions.

Particles: A finite- N algorithm is obtained by empirically approximating the mean-field control law. The particles $\{X_t^i : t \geq 0, 1 \leq i \leq N\}$ evolve according to:

$$dX_t^i = a(X_t^i) dt + \sigma(X_t^i) dB_t^i + K_t^{(N)}(X_t^i) \circ (dZ_t - \frac{h(X_t^i) + \hat{h}_t^{(N)}}{2} dt), \quad X_0^i \stackrel{\text{i.i.d.}}{\sim} p_0,$$

for $i = 1, \dots, N$, where $\{B_t^i : t \geq 0, 1 \leq i \leq N\}$ are mutually independent standard w.p., $\hat{h}_t^{(N)} := \frac{1}{N} \sum_{i=1}^N h(X_t^i)$ is the empirical approximation of \hat{h}_t , and $K_t^{(N)}$ is the output of an algorithm that approximates the solution to the Poisson equation (11) at each fixed time t :

$$\text{Gain function approximation: } K_t^{(N)} := \text{Algorithm}(\{X_t^i : 1 \leq i \leq N\}; h).$$

The notation is suggestive of the fact that algorithm is adapted to the ensemble $\{X_t^i : 1 \leq i \leq N\}$ and the function h ; the density $p_t(x)$ is not known in an explicit manner.

Two examples are presented in the sidebars to illustrate the FPF algorithm in practice: In the first example “Benefits of feedback”, analytical and numerical comparisons are provided to show how feedback control can help ameliorate the CoD. In the second example “FPF for SIR models” the FPF algorithm is applied to an epidemiological SIR model.

At this point, it is instructive to specialize FPF to the linear Gaussian case where the solution of the Poisson equation is explicitly known.

FPF for Linear Gaussian setting

Suppose $a(x) = Ax$, $h(x) = Hx$, and p_t is a Gaussian density with mean \bar{m}_t and variance $\bar{\Sigma}_t$. Then the solution of the Poisson equation is known in an explicit form [44, Sec. D]. The resulting gain function is constant and equal to the Kalman gain:

$$K_t(x) \equiv \bar{\Sigma}_t H^\top, \quad \forall x \in \mathbb{R}^d. \quad (12)$$

Therefore, the mean-field process (10) for the linear Gaussian problem is given as

$$d\bar{X}_t = A\bar{X}_t dt + d\bar{B}_t + \bar{\Sigma}_t H^\top (dZ_t - \frac{H\bar{X}_t + H\bar{m}_t}{2} dt), \quad \bar{X}_0 \sim p_0.$$

Given the explicit form of the gain function (12), the empirical approximation of the gain is simply $K_t^{(N)} = \Sigma_t^{(N)} H^\top$ where $\Sigma_t^{(N)}$ is the empirical covariance of the particles. Therefore, the evolution of the particles is:

$$dX_t^i = AX_t^i dt + dB_t^i + K_t^{(N)} (dZ_t - \frac{HX_t^i + Hm_t^{(N)}}{2} dt), \quad X_0^i \stackrel{\text{i.i.d.}}{\sim} p_0, \quad (13)$$

for $i = 1, \dots, N$, where $m_t^{(N)}$ is the empirical mean of the particles. The empirical quantities are computed as:

$$m_t^{(N)} := \frac{1}{N} \sum_{i=1}^N X_t^i, \quad \Sigma_t^{(N)} := \frac{1}{N-1} \sum_{i=1}^N (X_t^i - m_t^{(N)})(X_t^i - m_t^{(N)})^\top.$$

The linear Gaussian FPF (13) is identical to the square-root form of the ensemble Kalman filter (EnKF) [16, Eq. 3.3].

The main difficulty in implementing an FPF in general settings is the gain function approximation. Two algorithms for this problem are presented in the following section.

Gain function approximation

The exact gain function is a solution of the Poisson equation (11). In practice, this problem is solved numerically:

Input: samples $\{X^i : 1 \leq i \leq N\} \stackrel{\text{i.i.d.}}{\sim} \rho$, observation function $h(\cdot)$,

output: gain function $\{K(X^i) : 1 \leq i \leq N\}$,

where in filtering ρ is the (posterior) density at time t . The explicit dependence on time t is suppressed in this section. The problem is illustrated in Fig. 3.

Constant gain approximation

The simplest approximation is the *constant gain approximation* formula where the gain K_t is approximated by its expected value (which represents the best least-square approximation of the gain by a constant). Remarkably, the expected value admits a closed-form expression which is then readily approximated empirically using the particles:

$$\begin{aligned} \text{Const. gain approx: } \mathbb{E}[K_t(X_t)|\mathcal{Z}_t] &= \int_{\mathbb{R}^d} (h(x) - \hat{h}_t) x p_t(x) dx \\ &\approx \frac{1}{N} \sum_{i=1}^N (h(X_t^i) - \hat{h}_t^{(N)}) X_t^i. \end{aligned} \quad (14)$$

(See Figure 4 for an illustration of the constant gain approximation.) With the constant gain approximation, the FPF algorithm simplifies to an EnKF algorithm [10]. The constant gain formula (14) was known in the EnKF literature prior to the FPF derivation [48], [16].

There have been a number of studies to improve upon this formula [44], [9], [49], [50], [51], [52], [53]. In the following, we describe the diffusion map approximation which appears to be the most promising approach in general settings.

Diffusion map-based algorithm

The notation $e^{\epsilon\Delta_\rho}$ is used to denote the semigroup associated with the probability weighted Laplacian Δ_ρ [54]. As explained in the accompanying sidebar “Poisson equation and its approximations” (and more fully in [55]), the Poisson equation (11) is equivalently expressed as the fixed-point equation:

$$\phi = e^{\Delta_\rho\epsilon}\phi + \int_0^\epsilon e^{\Delta_\rho s}(h - \hat{h}) \, ds. \quad (15)$$

where $\epsilon > 0$ is arbitrary. For small values of ϵ , there is a well known approximation of the exact semigroup $e^{\Delta_\rho\epsilon}$ in terms of the so-called diffusion map:

$$T_\epsilon f(x) := \frac{1}{n_\epsilon(x)} \int_{\mathbb{R}^d} \frac{g_\epsilon(x-y)}{\sqrt{\int g_\epsilon(y-z)\rho(z) \, dz}} f(y)\rho(y) \, dy,$$

where $g_\epsilon(x) := e^{-\frac{|x|^2}{4\epsilon}}$ is the Gaussian kernel in \mathbb{R} and $n_\epsilon(x)$ is the normalization factor chosen so that $\int T_\epsilon 1(x) \, dx = 1$ [56].

It is straightforward to approximate the diffusion map empirically in terms of the particles:

$$T_\epsilon^{(N)} f(x) = \frac{1}{n_\epsilon^{(N)}(x)} \sum_{i=1}^N \frac{g_\epsilon(x-X^i)}{\sqrt{\sum_{j=1}^N g_\epsilon(X^i-X^j)}} f(X^i),$$

where $n_\epsilon^{(N)}(x)$ is the normalization factor.

Upon approximating the fixed-point equation (15) using the empirical approximation $T_\epsilon^{(N)}$ for $e^{\Delta_\rho\epsilon}$, one obtains the diffusion map-based algorithm. The algorithm is summarized in the sidebar “Diffusion map-based algorithm for gain function approximation”.

Error: bias variance trade-off

The error in diffusion map approximation comes from two sources: (i) the bias error due to the diffusion map approximation of the semigroup; (ii) the variance error due to empirical

approximation in terms of particles. The error is analyzed in [55] where it is shown that

$$\text{r.m.s.e} = \left(\mathbb{E} \left[\frac{1}{N} \sum_{i=1}^N |\mathbf{K}(X^i) - \mathbf{K}_{\text{exact}}(X^i)|^2 \right] \right)^{\frac{1}{2}} \leq \underbrace{O(\epsilon)}_{\text{bias}} + \underbrace{O\left(\frac{1}{\epsilon^{1+\frac{d}{2}} N^{\frac{1}{2}}}\right)}_{\text{variance}}. \quad (16)$$

The error due to bias converges to zero as $\epsilon \rightarrow 0$ and the error due to variance converges to zero as $N \rightarrow \infty$. There is trade-off between the two errors: To reduce bias, one must reduce ϵ . However, for any fixed value of N , one can reduce ϵ only up to a point where the variance starts increasing. The bias-variance trade-off is illustrated Fig. 5: If ϵ is large, the error due to bias dominates, while if ϵ is small, the error due to variance dominates.

As a final point, there is a remarkable and somewhat unexpected relationship between the diffusion map and the constant gain approximations. In particular, in the limit as $\epsilon \rightarrow \infty$, the diffusion map gain converges to the constant gain. This suggests a systematic procedure to improve upon the constant gain by de-tuning the value of ϵ away from the $[\epsilon = \infty]$ limit. For any fixed N , a finite value of ϵ is chosen to minimize the r.m.s.e. according to the bias variance trade-off. Based on this, a rule of thumb for choosing the ϵ value appears in [55, Remark 5.1].

Some Final Remarks

In the past decade, the coupling perspective to data assimilation problems has been enormously valuable with outstanding theoretical contributions and application impact. Given the limited scope of the present article with its narrow focus on the FPF algorithm, it is not possible to do justice to the depth and breadth of this exciting new area in one article. The reader is referred to the recent monograph [17] and the tutorial style review article [18] for an excellent introduction to the subject.

A few important remarks are also necessary at this point: The continuous-time formulation is stressed in this paper for the reasons of mathematical elegance and beauty. In practice, discrete-time formulations are much more common. The coupling viewpoint also applies to these settings [17] and was in fact also used in the paper to introduce the main ideas. Next, optimal couplings are almost always difficult to compute. Most popular forms of couplings used in practice are sub-optimal. This is true for the classical EnKF algorithm and also of the FPF algorithm. (A discussion on exactness and optimality for FPF appears in the sidebar.) As a final point, closely related to the coupling viewpoint is the gradient flow interpretation of the Bayes' update formula – see [46] for an FPF-specific exposition and also [57], [58] for related algorithms.

There are several directions for future work: It is an open problem to fully carry out the

stability and error analysis of the finite- N FPF particle system with the diffusion map-based gain function approximation. It will be very useful to be able to characterize the CoD in these general settings. It is also of interest to construct optimization type formulations that directly yield a finite- N algorithm without the need for empirical approximation as an intermediate step. Such constructions may lead to better error properties by design. Finally, apart from the optimal transportation formulation stressed in this paper, one may consider alternative approaches for control design. One possible direction is based on the Schrödinger bridge problem [59], [18].

References

- [1] S. B. Bastos and D. O. Cajueiro, “Modeling and forecasting the early evolution of the covid-19 pandemic in brazil,” *arXiv preprint arXiv:2003.14288*, 2020.
- [2] R. E. Kalman and R. S. Bucy, “New results in linear filtering and prediction theory,” *Journal of basic engineering*, vol. 83, no. 1, pp. 95–108, 1961.
- [3] H. A. P. Blom, “The continuous time roots of the interacting multiple model filter,” in *Proc. of the 51st IEEE Conf. Decision and Control*, Maui, Hawaii, Dec 2012, pp. 6015–6021.
- [4] Y. Bar-Shalom, F. Daum, and J. Huang, “The probabilistic data association filter,” *IEEE Control Syst. Mag.*, vol. 29, no. 6, pp. 82–100, Dec 2009.
- [5] A. Bensoussan, J. Frehse, P. Yam *et al.*, *Mean field games and mean field type control theory*. Springer, 2013, vol. 101.
- [6] R. Carmona and F. Delarue, *Probabilistic Theory of Mean Field Games with Applications I-II*. Springer, 2018.
- [7] T. Yang, P. G. Mehta, and S. P. Meyn, “A mean-field control-oriented approach for particle filtering,” in *Proc. of the 2011 American Control Conference*, San Francisco, June 2011, pp. 2037–2043.
- [8] —, “Feedback particle filter with mean-field coupling,” in *Proc. of 50th IEEE Conf. Decision and Control*, Orlando, FL, December 2011, pp. 7909–7916.
- [9] —, “Feedback particle filter,” *IEEE transactions on Automatic control*, vol. 58, no. 10, pp. 2465–2480, 2013.
- [10] A. Taghvaei, J. De Wiljes, P. G. Mehta, and S. Reich, “Kalman filter and its modern extensions for the continuous-time nonlinear filtering problem,” *Journal of Dynamic Systems, Measurement, and Control*, vol. 140, no. 3, p. 030904, 2018.
- [11] T. Yang, G. Huang, and P. G. Mehta, “Joint probabilistic data association-feedback particle filter for multiple target tracking applications,” in *2012 American Control Conference (ACC)*. IEEE, 2012, pp. 820–826.
- [12] T. Yang, H. A. Blom, and P. G. Mehta, “Interacting multiple model-feedback particle filter for stochastic hybrid systems,” in *52nd IEEE Conference on Decision and Control*. IEEE,

2013, pp. 7065–7070.

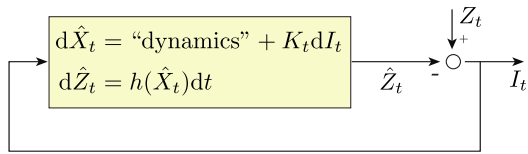
- [13] G. Evensen, “Sequential data assimilation with a nonlinear quasi-geostrophic model using Monte Carlo methods to forecast error statistics,” *Journal of Geophysical Research: Oceans*, vol. 99, no. C5, pp. 10 143–10 162, 1994.
- [14] D. Crisan and J. Xiong, “Approximate McKean-Vlasov representations for a class of SPDEs,” *Stochastics*, vol. 82, no. 1, pp. 53–68, 2010.
- [15] S. Reich, “A dynamical systems framework for intermittent data assimilation,” *BIT Numerical Analysis*, vol. 51, pp. 235–249, 2011.
- [16] K. Bergemann and S. Reich, “An ensemble Kalman-Bucy filter for continuous data assimilation,” *Meteorologische Zeitschrift*, vol. 21, no. 3, pp. 213–219, 2012.
- [17] S. Reich and C. Cotter, *Probabilistic forecasting and Bayesian data assimilation*. Cambridge University Press, 2015.
- [18] S. Reich, “Data assimilation: The Schrödinger perspective,” *Acta Numerica*, vol. 28, pp. 635–711, 2019.
- [19] Y. Cheng and S. Reich, “A McKean optimal transportation perspective on Feynman-Kac formulae with application to data assimilation,” *arXiv preprint arXiv:1311.6300*, 2013. [Online]. Available: <https://arxiv.org/abs/1311.6300>
- [20] N. J. Gordon, D. J. Salmond, and A. F. Smith, “Novel approach to nonlinear/non-Gaussian Bayesian state estimation,” in *IEE Proceedings F (Radar and Signal Processing)*, vol. 140, 1993, pp. 107–113.
- [21] A. M. Doucet, A. and Johansen, “A tutorial on particle filtering and smoothing: Fifteen years later,” *Handbook of Nonlinear Filtering*, vol. 12, pp. 656–704, 2009. [Online]. Available: https://www.cs.ubc.ca/~arnaud/doucet_johansen_tutorialPF.pdf
- [22] P. Del Moral and A. Guionnet, “On the stability of interacting processes with applications to filtering and genetic algorithms,” in *Annales de l’Institut Henri Poincaré (B) Probability and Statistics*, vol. 37, no. 2. Elsevier, 2001, pp. 155–194.
- [23] O. Cappé, E. Moulines, and T. Rydén, “Inference in hidden markov models,” in *Proceedings of EUSFLAT Conference*, 2009, pp. 14–16.
- [24] T. Bengtsson, P. Bickel, and B. Li, “Curse of dimensionality revisited: Collapse of the particle filter in very large scale systems,” in *IMS Lecture Notes - Monograph Series in Probability and Statistics: Essays in Honor of David F. Freedman*. Institute of Mathematical Sciences, 2008, vol. 2, pp. 316–334.
- [25] A. Beskos, D. Crisan, A. Jasra, and N. Whiteley, “Error bounds and normalising constants for sequential Monte Carlo samplers in high dimensions,” *Advances in Applied Probability*, vol. 46, no. 1, pp. 279–306, 2014.
- [26] P. Rebeschini, R. Van Handel *et al.*, “Can local particle filters beat the curse of dimensionality?” *The Annals of Applied Probability*, vol. 25, no. 5, pp. 2809–2866, 2015.

- [27] P. Del Moral, “Feynman-Kac formulae,” in *Feynman-Kac Formulae*. Springer, 2004, pp. 47–93.
- [28] A. Bain and D. Crisan, *Fundamentals of stochastic filtering*. Springer, 2009, vol. 3.
- [29] C. Villani, *Topics in optimal transportation*. American Mathematical Soc., 2003, no. 58.
- [30] L. C. Evans, “Partial differential equations and Monge-Kantorovich mass transfer,” *Current developments in mathematics*, pp. 65–126, 1997.
- [31] A. Taghvaei and P. G. Mehta, “An optimal transport formulation of the linear feedback particle filter,” in *American Control Conference (ACC), 2016*. IEEE, 2016, pp. 3614–3619.
- [32] J. Whitaker and T. M. Hamill, “Ensemble data assimilation without perturbed observations,” *Monthly Weather Review*, vol. 130, no. 7, pp. 1913–1924, 2002.
- [33] J. Mandel, L. Cobb, and J. D. Beezley, “On the convergence of the ensemble Kalman filter,” *Applications of Mathematics*, vol. 56, no. 6, pp. 533–541, 2011.
- [34] P. Del Moral and J. Tugaut, “On the stability and the uniform propagation of chaos properties of ensemble Kalman–Bucy filters,” *Ann. Appl. Probab.*, vol. 28, no. 2, pp. 790–850, 04 2018. [Online]. Available: <https://doi.org/10.1214/17-AAP1317>
- [35] P. Del Moral, A. Kurtzmann, and J. Tugaut, “On the stability and the uniform propagation of chaos of a class of extended ensemble Kalman–Bucy filters,” *SIAM Journal on Control and Optimization*, vol. 55, no. 1, pp. 119–155, 2017.
- [36] J. de Wiljes, S. Reich, and W. Stannat, “Long-time stability and accuracy of the ensemble Kalman–Bucy filter for fully observed processes and small measurement noise,” *SIAM Journal on Applied Dynamical Systems*, vol. 17, no. 2, pp. 1152–1181, 2018.
- [37] A. Taghvaei and P. G. Mehta, “An optimal transport formulation of the ensemble kalman filter,” *ArXiv (To appear in Transactions of Automatic Control (TAC))*, vol. abs/1910.02338, 2019.
- [38] A. Sznitman, “Topics in propagation of chaos,” *Ecole d’Eté de Probabilités de Saint-Flour XIX—1989*, pp. 165–251, 1991.
- [39] S. T. Rachev and L. Rüschendorf, *Mass Transportation Problems: Volume I: Theory*. Springer Science & Business Media, 1998, vol. 1.
- [40] T. A. El Moselhy and Y. M. Marzouk, “Bayesian inference with optimal maps,” *Journal of Computational Physics*, vol. 231, no. 23, pp. 7815–7850, 2012.
- [41] D. A. Mesa, J. Tantiengloc, M. Mendoza, S. Kim, and T. P. Coleman, “A distributed framework for the construction of transport maps,” *Neural computation*, vol. 31, no. 4, pp. 613–652, 2019.
- [42] J. Heng, A. Doucet, and Y. Pokern, “Gibbs flow for approximate transport with applications to Bayesian computation,” *arXiv preprint arXiv:1509.08787*, 2015. [Online]. Available: <https://arxiv.org/abs/1509.08787>

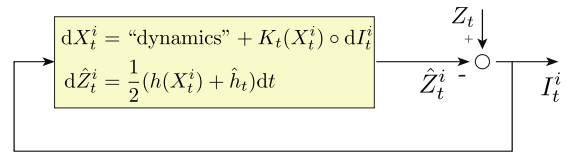
- [43] B. Oksendal, *Stochastic differential equations: an introduction with applications*. Springer Science & Business Media, 2013.
- [44] T. Yang, R. S. Laugesen, P. G. Mehta, and S. P. Meyn, “Multivariable feedback particle filter,” *Automatica*, vol. 71, pp. 10–23, 2016.
- [45] S. Pathiraja, S. Reich, and W. Stannat, “McKean-vlasov sdes in nonlinear filtering,” *arXiv preprint arXiv:2007.12658*, 2020.
- [46] R. S. Laugesen, P. G. Mehta, S. P. Meyn, and M. Raginsky, “Poisson’s equation in nonlinear filtering,” *SIAM Journal on Control and Optimization*, vol. 53, no. 1, pp. 501–525, 2015. [Online]. Available: [10.1137/13094743X](https://doi.org/10.1137/13094743X)
- [47] C. Zhang, A. Taghvaei, and P. G. Mehta, “Feedback particle filter on riemannian manifolds and matrix lie groups,” *IEEE Transactions on Automatic Control*, vol. 63, no. 8, pp. 2465–2480, 2017.
- [48] G. Evensen, *Data Assimilation. The Ensemble Kalman Filter*. New York: Springer-Verlag, 2006.
- [49] K. Berntorp and P. Grover, “Data-driven gain computation in the feedback particle filter,” in *2016 American Control Conference (ACC)*, 2016, pp. 2711–2716.
- [50] Y. Matsuura, R. Ohata, K. Nakakuki, and R. Hirokawa, “Suboptimal gain functions of feedback particle filter derived from continuation method,” in *AIAA Guidance, Navigation, and Control Conference*, 2016, p. 1620.
- [51] A. Radhakrishnan, A. Devraj, and S. Meyn, “Learning techniques for feedback particle filter design,” in *Conference on Decision and Control (CDC), 2016*. IEEE, 2016, pp. 648–653.
- [52] A. Radhakrishnan and S. Meyn, “Feedback particle filter design using a differential-loss reproducing kernel Hilbert space,” in *2018 Annual American Control Conference (ACC)*. IEEE, 2018, pp. 329–336.
- [53] K. Berntorp, “Comparison of gain function approximation methods in the feedback particle filter,” in *2018 21st International Conference on Information Fusion (FUSION)*. IEEE, 2018, pp. 123–130.
- [54] D. Bakry, I. Gentil, and M. Ledoux, *Analysis and geometry of Markov diffusion operators*. Springer Science & Business Media, 2013, vol. 348.
- [55] A. Taghvaei, P. G. Mehta, and S. P. Meyn, “Diffusion map-based algorithm for gain function approximation in the feedback particle filter,” *SIAM/ASA Journal on Uncertainty Quantification*, vol. 8, no. 3, pp. 1090–1117, 2020.
- [56] R. R. Coifman and S. Lafon, “Diffusion maps,” *Applied and computational harmonic analysis*, vol. 21, no. 1, pp. 5–30, 2006.
- [57] A. Halder and T. T. Georgiou, “Gradient flows in filtering and Fisher-Rao geometry,” in *2018 Annual American Control Conference (ACC)*. IEEE, 2018, pp. 4281–4286.

- [58] A. Garbuno-Inigo, F. Hoffmann, W. Li, and A. M. Stuart, “Interacting langevin diffusions: Gradient structure and ensemble kalman sampler,” *SIAM Journal on Applied Dynamical Systems*, vol. 19, no. 1, pp. 412–441, 2020.
- [59] Y. Chen, T. T. Georgiou, and M. Pavon, “On the relation between optimal transport and Schrödinger bridges: A stochastic control viewpoint,” *Journal of Optimization Theory and Applications*, vol. 169, no. 2, pp. 671–691, 2016.
- [60] P. Bickel, B. Li, T. Bengtsson *et al.*, “Sharp failure rates for the bootstrap particle filter in high dimensions,” in *Pushing the limits of contemporary statistics: Contributions in honor of Jayanta K. Ghosh*. Institute of Mathematical Statistics, 2008, pp. 318–329.
- [61] T. Bengtsson, P. Bickel, and B. Li, “Curse of dimensionality revisited: Collapse of the particle filter in very large scale systems,” in *IMS Lecture Notes - Monograph Series in Probability and Statistics: Essays in Honor of David F. Freedman*. Institute of Mathematical Sciences, 2008, vol. 2, pp. 316–334.
- [62] C. Snyder, T. Bengtsson, P. Bickel, and J. Anderson, “Obstacles to high-dimensional particle filtering,” *Monthly Weather Review*, vol. 136, no. 12, pp. 4629–4640, 2008.
- [63] S. C. Surace, A. Kutschireiter, and J.-P. Pfister, “How to avoid the curse of dimensionality: scalability of particle filters with and without importance weights,” *Siam Review*, vol. 61, no. 1, pp. 79–91, 2019.
- [64] S. Y. Olmez, A. Taghvaei, and P. G. Mehta, “Deep fpf: Gain function approximation in high-dimensional setting,” *arXiv preprint arXiv:2010.01183*, 2020.
- [65] E. Weinan and B. Yu, “The deep ritz method: a deep learning-based numerical algorithm for solving variational problems,” *Communications in Mathematics and Statistics*, vol. 6, no. 1, pp. 1–12, 2018.
- [66] W. C. Roda, M. B. Varughese, D. Han, and M. Y. Li, “Why is it difficult to accurately predict the covid-19 epidemic?” *Infectious Disease Modelling*, 2020.
- [67] S. L. Wu, A. N. Mertens, Y. S. Crider, A. Nguyen, N. N. Pokpongkiat, S. Djajadi, A. Seth, M. S. Hsiang, J. M. Colford, A. Reingold *et al.*, “Substantial underestimation of sars-cov-2 infection in the united states,” *Nature communications*, vol. 11, no. 1, pp. 1–10, 2020.
- [68] R. Li, S. Pei, B. Chen, Y. Song, T. Zhang, W. Yang, and J. Shaman, “Substantial undocumented infection facilitates the rapid dissemination of novel coronavirus (sars-cov-2),” *Science*, vol. 368, no. 6490, pp. 489–493, 2020.
- [69] M. G. M. Gomes, R. Aguas, R. M. Corder, J. G. King, K. E. Langwig, C. Souto-Maior, J. Carneiro, M. U. Ferreira, and C. Penha-Goncalves, “Individual variation in susceptibility or exposure to sars-cov-2 lowers the herd immunity threshold,” *medRxiv*, 2020.
- [70] P. E. Paré, C. L. Beck, and T. Basar, “Modeling, estimation, and analysis of epidemics over networks: An overview,” *Annual Reviews in Control: Special Issue on Systems and Control Research Efforts Against COVID-19 and Future Pandemics*, 2020.

- [71] S. Y. Olmez, J. Mori, E. Miehl, T. Basar, R. L. Smith, M. West, and P. Mehta, “A data-informed approach for analysis, validation, and identification of covid-19 models,” *medRxiv*, 2020. [Online]. Available: <https://www.medrxiv.org/content/early/2020/10/06/2020.10.03.20206250.1>
- [72] R. Engbert, M. M. Rabe, R. Kliegl, and S. Reich, “Sequential data assimilation of the stochastic seir epidemic model for regional covid-19 dynamics,” *medRxiv*, 2020.
- [73] G. Evensen, J. Amezcua, M. Bocquet, A. Carrassi, A. Farchi, A. Fowler, P. Houtekamer, C. K. Jones, R. de Moraes, M. Pulido *et al.*, “An international assessment of the covid-19 pandemic using ensemble data assimilation,” *medRxiv*, 2020.



(a) Kalman filter



(b) Feedback particle filter

Figure 1: Feedback control structure of the Kalman filter and the feedback particle filter (FPF). \hat{X}_t in the KF is the estimate (conditional mean) of the hidden state. X_t^i in the FPF is a sample from the posterior (conditional distribution) of the hidden state. In either algorithms, the Bayesian update is implemented via a gain times error control law.

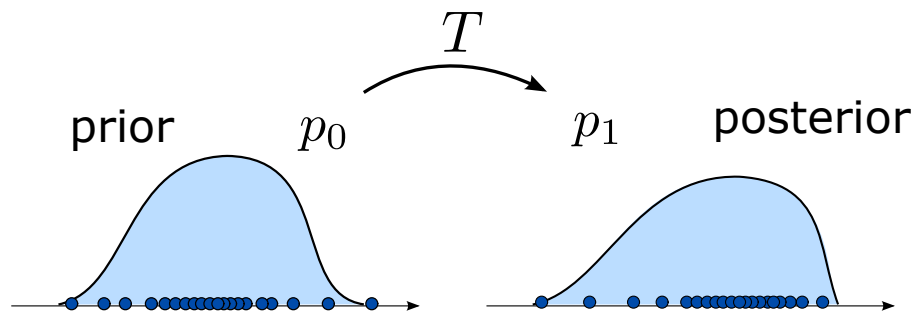


Figure 2: Coupling viewpoint of the filtering problem. The task of a particle filter is to convert a sample of N particles from the prior distribution to a sample of N particles from the posterior distribution. This task is viewed as finding a coupling between the prior and the posterior distributions.

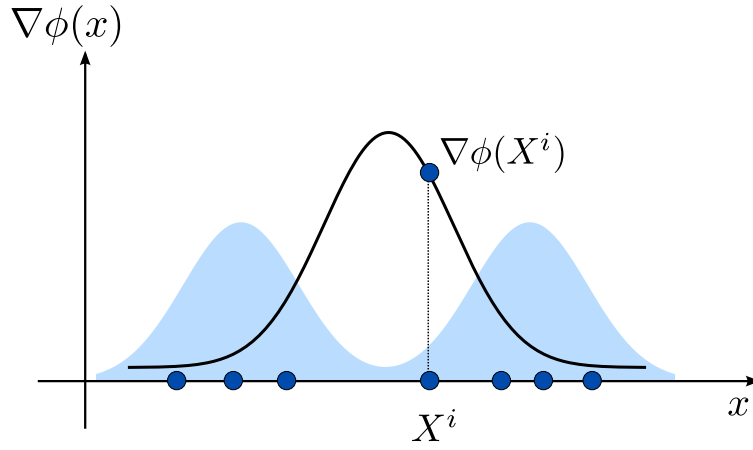


Figure 3: Gain function approximation problem in the feedback particle filter. The exact gain function $K(x) = \nabla\phi(x)$ where ϕ solves the Poisson equation (11). The numerical problem is to approximate $\nabla\phi(x)|_{x=X^i}$ using only the particles $\{X^i : 1 \leq i \leq N\}$ sampled from density ρ (depicted as shaded region).

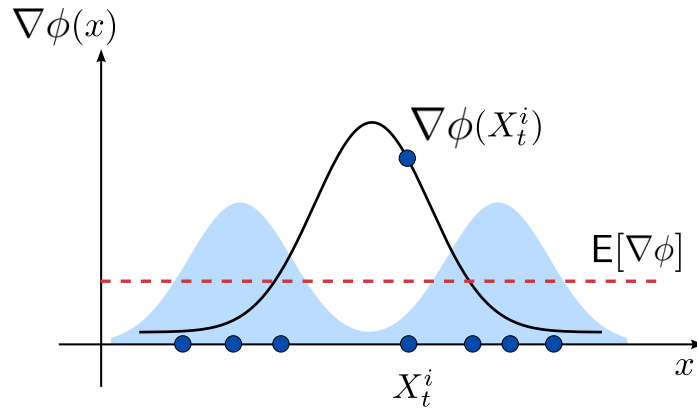
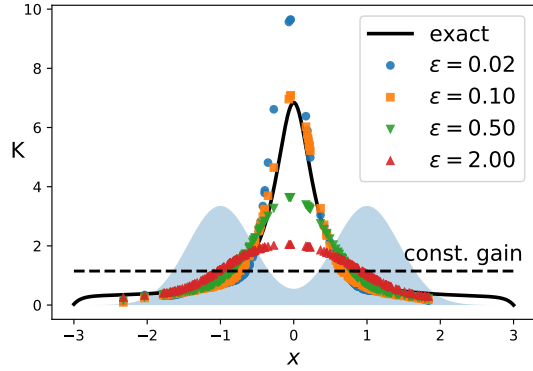
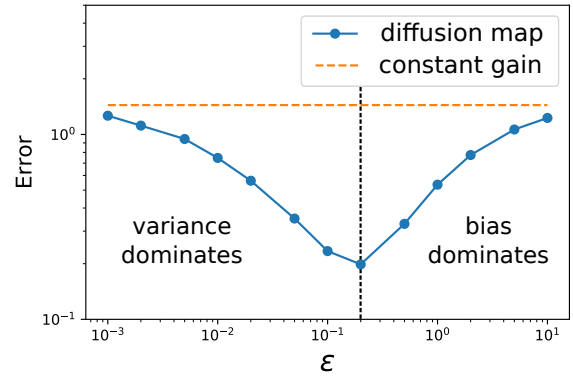


Figure 4: Constant gain approximation in the feedback particle filter. The gain function is approximated by its expected value according to (14).



(a) Approximate gain function compared to the exact gain function (solid line),



(b) The root mean squared error as a function of the parameter ϵ .

Figure 5: Bias variance trade-off in diffusion map-based gain function approximation. (a) The dashed line is the constant gain solution (14). As $\epsilon \rightarrow \infty$, the diffusion map gain converges to the constant gain. (The shaded area in the background is the density function ρ taken as sum of two Gaussians $\mathcal{N}(-1, \sigma^2)$ and $\mathcal{N}(+1, \sigma^2)$ with $\sigma^2 = 0.2$. The exact gain function $K(x)$ is computed for $h(x) = x$ by using an integral formula [55, Eq. 4.6].) (b) The r.m.s.e. is computed as an empirical approximation of (16) by averaging over 1000 simulations for $N = 200$ particles.

Summary

Feedback particle filter (FPF) is a Monte-Carlo (MC) algorithm to approximate the solution of a stochastic filtering problem. In contrast to conventional particle filters, the Bayesian update step in FPF is implemented via a mean-field type feedback control law.

The objective for this paper is to situate the development of FPF and related controlled interacting particle system algorithms within the framework of optimal transportation theory. Starting from the simplest setting of the Bayes' update formula, a coupling viewpoint is introduced to construct particle filters. It is shown that the conventional importance sampling resampling particle filter implements an independent coupling. Design of optimal couplings is introduced first for the simple Gaussian settings and subsequently extended to derive the FPF algorithm. The final half of the paper provides a review of some of the salient aspects of the FPF algorithm including the feedback structure, algorithms for gain function design, and comparison with conventional particle filters. The comparison serves to illustrate the benefit of feedback in particle filtering.

Summary of the linear Gaussian example

The formulae for the linear Gaussian example are summarized as follows:

Prior: Gaussian $\mathcal{N}(m_0, \Sigma_0)$

Observation model: $Y = HX + W$

Likelihood function: $l(x) = \exp(-\frac{|y - Hx|^2}{2})$

Posterior: Gaussian $\mathcal{N}(m_1, \Sigma_1)$

Optimal transport map: $T(x) = F(x - m_0) + m_1$

Mean-field process: $\bar{X}_1 = F(\bar{X}_0 - m_0) + m_0 + K(Y - Hm_0)$

Particle system: $X_1^i = F^{(N)}(X_0^i - m_0^{(N)}) + m_0^{(N)} + K^{(N)}(Y - Hm_0^{(N)}), \quad \text{for } i = 1, \dots, N$

Optimal transport construction of stochastic processes

Deterministic path

Let $\mathcal{P}_2(\mathbb{R}^d)$ be the space of everywhere positive probability densities on \mathbb{R}^d with finite second moment. Given a smooth path $\{p_t \in \mathcal{P}_2(\mathbb{R}^d) : t \geq 0\}$ the problem is to construct a stochastic process $\{\bar{X}_t; t \geq 0\}$ such that the probability density of \bar{X}_t , denoted as \bar{p}_t , equals p_t for all $t \geq 0$. The exactness condition is expressed as

$$\bar{p}_t = p_t, \quad \forall t \geq 0. \quad (\text{S1})$$

Now, there are infinitely many stochastic processes that satisfy the exactness condition. This is because the exactness condition specifies only the one-time marginal distribution which is clearly not enough to uniquely identify the stochastic process, e.g., the two-time joint distributions are not specified. A unique choice is made by prescribing an additional optimality criterion based on the optimal transportation theory.

To make these considerations concrete, assume that the given path $\{p_t : t \geq 0\}$ evolves according to the PDE

$$\frac{\partial p_t}{\partial t} = \mathcal{V}(p_t),$$

where $\mathcal{V}(\cdot)$ is an operator (e.g., the Laplacian) that acts on probability densities. (This necessarily restricts the operator \mathcal{V} , e.g., $\int \mathcal{V}(p)(x) dx = 0$ for all $p \in \mathcal{P}_2(\mathbb{R}^d)$.) The following model is assumed for the process $\{\bar{X}_t : t \geq 0\}$:

$$\frac{d}{dt} \bar{X}_t = u_t(\bar{X}_t), \quad \bar{X}_0 \sim p_0, \quad (\text{S2})$$

where $u_t(\cdot)$ is a control law that needs to be designed. Using the continuity equation, the exactness condition (S1) will be satisfied if

$$-\nabla \cdot (\bar{p}_t u_t) = \mathcal{V}(\bar{p}_t), \quad \forall t \geq 0. \quad (\text{S3})$$

The non-uniqueness issue is now readily seen: The first-order PDE (S3) admits infinitely many solutions. A unique solution u_t is picked by optimizing the coupling between \bar{X}_t and $\bar{X}_{t+\Delta t}$ in the limit as $\Delta t \rightarrow 0$. The leading term in the transportation cost $\mathbb{E}[|X_{t+\Delta t} - X_t|^2]$ is of order $O(\Delta t^2)$ whereby

$$\lim_{\Delta t \rightarrow 0} \frac{1}{\Delta t^2} \mathbb{E}[|X_{t+\Delta t} - X_t|^2] = \int_{\mathbb{R}^d} |u_t(x)|^2 \bar{p}_t(x) dx.$$

Therefore, for each fixed $t \in [0, 1]$, the control law u_t is obtained by solving the constrained optimization problem

$$\min_{u_t} \int_{\mathbb{R}^d} |u_t(x)|^2 \bar{p}_t(x) dx, \quad \text{s.t.} \quad -\nabla \cdot (\bar{p}_t u_t) = \mathcal{V}(\bar{p}_t). \quad (\text{S4})$$

The cost is the infinitesimal form of the L^2 -Wasserstein distance and the constraint expresses the exactness condition.

By a standard calculus of variation argument, the solution of the optimization problem (S4) is obtained as $u_t^* = \nabla \phi_t$ where ϕ_t solves the second-order PDE $-\nabla \cdot (\bar{p}_t \nabla \phi_t) = \mathcal{V}(\bar{p}_t)$. The resulting stochastic process \bar{X}_t evolves according to

$$\begin{aligned} \frac{d\bar{X}_t}{dt} &= \nabla \phi_t(\bar{X}_t), \quad \bar{X}_0 \sim p_0, \\ \phi_t \text{ solves the PDE } &-\nabla \cdot (\bar{p}_t \nabla \phi_t) = \mathcal{V}(\bar{p}_t). \end{aligned}$$

As a concrete example, suppose the given path is a solution of the heat equation $\frac{\partial p_t}{\partial t} = \Delta p_t$. (So $\mathcal{V}(\cdot)$ is the Laplacian operator.) The solution of the second-order PDE is easily obtained as $\phi_t = \log(\bar{p}_t)$. The optimal transport process \bar{X}_t then evolves according to

$$\frac{d}{dt} \bar{X}_t = -\nabla \log(p_t(\bar{X}_t)), \quad \bar{X}_0 \sim p_0.$$

This process should be compared to the SDE

$$dX_t = dB_t, \quad X_0 \sim p_0, \tag{S5}$$

where $\{B_t : t \geq 0\}$ is a w.p.. The SDE (S5) is a well-known stochastic coupling whose one-point marginal evolves according to the solution of the heat equation.

Stochastic path

In the filtering problem, the path of the posterior probability densities is stochastic (because it depends upon random observations $\{Z_t : t \geq 0\}$). Therefore, the preceding discussion is not directly applicable. Suppose the stochastic path $\{p_t(\cdot) \in \mathcal{P}_2(\mathbb{R}^d) : t \geq 0\}$ is governed by a stochastic PDE

$$dp_t = \mathcal{H}(p_t) dI_t,$$

where $\mathcal{H}(\cdot)$ is an operator that acts on probability densities and $\{I_t : t \geq 0\}$ is a w.p..

Consider the following SDE model:

$$d\bar{X}_t = u_t(\bar{X}_t) dt + K_t(\bar{X}_t) dI_t, \quad \bar{X}_0 \sim p_0,$$

where, compared to the deterministic form of (S2), an additional stochastic term is now included. The problem is to identify control laws $u_t(\cdot)$ and $K_t(\cdot)$ such that the conditional distribution of \bar{X}_t equals p_t . This exactness condition, counterpart of (S3), now is

$$-\nabla \cdot (\bar{p}_t K_t) = \mathcal{H}(\bar{p}_t), \tag{S6a}$$

$$-\nabla \cdot (\bar{p}_t u_t) + \frac{1}{2}(\nabla \cdot (\bar{p}_t K_t) K_t + \bar{p}_t K_t \nabla K_t) = 0. \tag{S6b}$$

These equations are obtained by writing the time-evolution of the conditional probability density of \bar{X}_t [44, Prop. 1]. As in the deterministic setting, the solution is not unique.

The unique optimal control law is obtained by requiring that the coupling between \bar{X}_t and $\bar{X}_{t+\Delta t}$ is optimal in the limit as $\Delta t \rightarrow 0$. In contrast to the deterministic setting, the leading term in the transportation cost $\mathbb{E}[|X_{t+\Delta t} - X_t|^2]$ is of order $O(\Delta t)$ whereby

$$\lim_{\Delta t \rightarrow 0} \frac{1}{\Delta t} \mathbb{E}[|X_{t+\Delta t} - X_t|^2] = \int_{\mathbb{R}^d} |K_t(x)|^2 \bar{p}_t(x) dx. \quad (\text{S7})$$

Therefore, for each fixed $t \in [0, 1]$, the control law K_t is obtained by solving the constrained optimization problem

$$\min_{K_t} \int_{\mathbb{R}^d} |K_t(x)|^2 \bar{p}_t(x) dx, \quad \text{s.t.} \quad -\nabla \cdot (\bar{p}_t K_t) = \mathcal{H}_t(\bar{p}_t). \quad (\text{S8})$$

As before, the solution of the optimization problem (S8) is given by $K_t^* = \nabla \phi_t$ where ϕ_t solves the second-order PDE $-\nabla \cdot (\bar{p}_t \nabla \phi_t) = \mathcal{H}(\bar{p}_t)$.

It remains to identify the control law for u_t . For this purpose, the second-order term in the infinitesimal Wasserstein cost is used:

$$\lim_{\Delta t \rightarrow 0} \frac{1}{\Delta t^2} \left(\mathbb{E}[|X_{t+\Delta t} - X_t|^2] - \Delta t \int_{\mathbb{R}^d} |K_t^*|^2 \bar{p}_t dx \right) = \int_{\mathbb{R}^d} |u_t|^2 \bar{p}_t dx.$$

The righthand-side is minimized subject to the constraint (S6b). Remarkably, the optimal solution is expressed as

$$u_t^* = -\frac{1}{2\bar{p}_t} \mathcal{H}(\bar{p}_t) \nabla \phi_t + \frac{1}{2} \nabla^2 \phi_t \nabla \phi_t + \xi_t,$$

where ξ_t is the (unique such) divergence free vector field (i.e., $\nabla \cdot (p_t \xi_t) = 0$) such that u_t is of a gradient form. The resulting optimal transport process is

$$d\bar{X}_t = \nabla \phi_t(\bar{X}_t) \circ (dI_t - \frac{1}{2\bar{p}_t} \mathcal{H}(\bar{p}_t) dt) + \xi_t(\bar{X}_t) dt, \quad \bar{X}_0 \sim p_0. \quad (\text{S9})$$

It is also readily shown that the process $\{\bar{X}_t : t \geq 0\}$ is in fact exact for any choice of divergence free vector field ξ_t . The most convenient such choice is obtained by simply setting $\xi_t \equiv 0$. The resulting filter is exact and furthermore also (infinitesimally) optimal to the first-order (see (S7)).

For the special case of the nonlinear filtering problem, $\mathcal{H}(p) = (h - \hat{h})p$ where $\hat{h} = \int h(x)p(x) dx$ and $dI_t = dZ_t - \hat{h}_t dt$ is the increment of the innovation process. The optimal transport stochastic process (S9) is then given by the Stratonovich form

$$d\bar{X}_t = \nabla \phi_t(\bar{X}_t) \circ (dZ_t - \frac{1}{2}(h + \hat{h}_t) dt) + \xi_t(\bar{X}_t) dt, \quad \bar{X}_0 \sim p_0.$$

The control law in the FPF algorithm (10) represents the particular sub-optimal choice $\xi_t \equiv 0$.

Benefit of Feedback

In this sidebar, we consider a simple example to highlight the phenomena of curse of dimensionality (CoD) in particle filters and provide comparison with FPF to see how the curse is mitigated by using feedback control. The example we consider is as follows:

$$dX_t = 0, \quad X_0 \sim \mathcal{N}(0, \sigma_0^2 I_d), \quad (\text{S10a})$$

$$dZ_t = X_t dt + \sigma_w dW_t, \quad (\text{S10b})$$

for $t \in [0, 1]$, where X_t is a d -dimensional process, $\sigma_w, \sigma_0 > 0$ and I_d is a $d \times d$ identity matrix. The posterior distribution at time $t = 1$ is a Gaussian distribution $\mathcal{N}(m_1, \Sigma_1)$ with mean $m_1 = \frac{\sigma_0^2}{\sigma_0^2 + \sigma_w^2}$ and variance $\Sigma_1 = \frac{\sigma_0^2 \sigma_w^2}{\sigma_0^2 + \sigma_w^2} I_d$.

We consider the following MC approaches to approximate the posterior distribution:

- 1) SIR particle filter (PF): Sample $\{X_0^i : 1 \leq i \leq N\}$ from the initial distribution. Form the weighted distribution and generate new samples from the weighted distribution.

$$X_1^i \sim \sum_{i=1}^N w_i \delta_{X_0^i}, \quad w_i = \frac{e^{-\frac{|Z_1 - X_0^i|^2}{2\sigma_w^2}}}{\mathbb{E}[e^{-\frac{|Z_1 - X_0^i|^2}{2\sigma_w^2}} | \mathcal{Z}_1]}, \quad X_0^i \sim \mathcal{N}(0, \sigma_0^2 I_d). \quad (\text{S11})$$

- 2) Feedback particle filter (FPF): Simulate the particles according to

$$dX_t^i = \frac{1}{\sigma_w^2} \Sigma_t^{(N)} \left(dZ_t - \frac{X_t^i + m_t^{(N)}}{2} dt \right), \quad X_0^i \sim \mathcal{N}(0, \sigma_0^2 I_d). \quad (\text{S12})$$

for $t \in [0, 1]$, where $m_t^{(N)}$ is the empirical mean of the particles, and $\Sigma_t^{(N)}$ is the empirical variance of the particles.

We compare the mean squared error (m.s.e) in approximating the exact conditional mean m_1 of X_1 . The m.s.e is defined as

$$\text{m.s.e} := \mathbb{E} \left[\frac{1}{N} \sum_{i=1}^N |X_1^i - m_1|^2 \right].$$

In [37], the following is proved:

Proposition 1: Consider the filtering problem (S10) with state dimension d . Then

- (i) For the PF (S11)

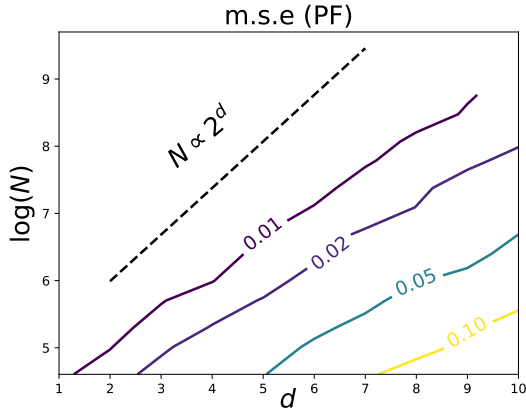
$$\text{m.s.e}_{\text{PF}}(f) = \frac{\sigma^2}{N} \left(3(2^d) - \frac{1}{2} \right) \geq \frac{\sigma^2}{N} 2^{d+1}.$$

(ii) For the FPF (S12)

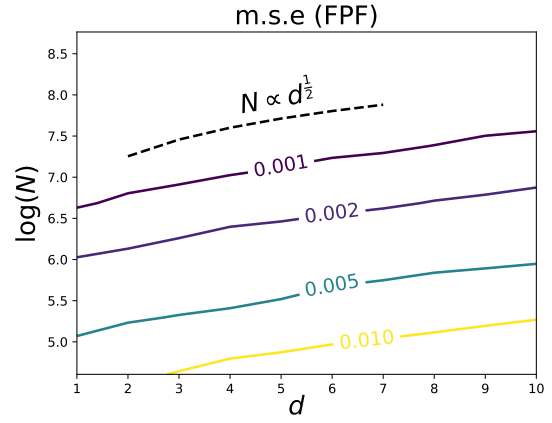
$$\text{m.s.e}_{\text{FPF}}(f) \leq \frac{\sigma^2}{N}(3d^2 + 2d).$$

The result above is consistent with the extensive studies on importance sampling-based particle filters [60], [61], [62], [26]. In these papers, it is shown that if $\frac{\log N \log d}{d} \rightarrow 0$ then the largest importance weight $\max_{1 \leq i \leq N} w^i \rightarrow 1$ in probability. Consequently, in order to prevent the weight collapse, the number of particles must grow exponentially with the dimension. This phenomenon is referred to as the curse of dimensionality (CoD) for the particle filters.

A numerical comparison of the m.s.e. as a function of N and d is depicted in Figure S1-(a)-(b). The expectation is approximated by averaging over $M = 1000$ independent simulations. It is observed that, in order to have the same error, the importance sampling-based approach requires the number of samples N to grow exponentially with the dimension d , whereas the growth using the FPF for this numerical example is $O(d^{\frac{1}{2}})$. The scaling with dimension depicted in Figure S1 (b) suggests that the $O(d^2)$ bound for the m.s.e in the linear FPF is loose. This is because of the conservative nature of approximations used in deriving the inequality [37]. The overall conclusions of the study are consistent with other numerical results reported in the literature [63].



(a) importance sampling particle filter (PF) (S11)



(b) feedback particle filter (FPF) (S12)

Figure S1: Overcoming the curse of dimensionality of particle filters. The solid lines correspond to the level sets of the mean squared error for the filtering problem (S10). In order to have the same error, the PF requires the number of samples N to grow exponentially with the dimension d , whereas the growth using the FPF for this numerical example is $O(d^{1/2})$.

Poisson equation and its approximations

The Poisson equation (11) of nonlinear filtering is a linear PDE. Its finite-dimensional counterpart is a familiar linear problem

$$Ax = b, \tag{S13}$$

where A is a $n \times n$ (strictly) positive-definite symmetric matrix and the righthand-side b is a given $n \times 1$ vector. The problem is to obtain the unknown $n \times 1$ vector x . For this purpose, the following equivalent formulations of the finite-dimensional problem are first introduced:

- 1) x is the solution of the weak form

$$y^\top Ax = y^\top b, \quad \forall y \in \mathbb{R}^n.$$

- 2) For any $t > 0$, x is the solution to the fixed-point equation

$$x = e^{-tA}x + \int_0^t e^{-sA}b \, ds.$$

- 3) x is the solution of the optimization problem

$$\min_{x \in \mathbb{R}^n} \frac{1}{2} x^\top Ax - x^\top b.$$

When n is large, these formulations are useful to numerically approximate the solution of (S13):

- 1) For each fixed $y \in \mathbb{R}^n$, the weak form is a single equation. By restricting y to a suitable low-dimensional subspace $S \subset \mathbb{R}^n$, the number of linear equations is reduced for the purposes of obtaining an approximate solution (possibly also in S).
- 2) The fixed-point equation form is useful because e^{-tA} is a contraction for positive-definite A . So, a good initial guess for x can readily be improved by using the Banach iteration.
- 3) The optimization form is useful to develop alternate (e.g., search type) algorithms to obtain the solution to (S13).

We turn our attention next to the Poisson equation (11) expressed succinctly as

$$-\Delta_\rho \phi = h - \hat{h},$$

where $\Delta_\rho = \frac{1}{\rho} \nabla \cdot (\rho \nabla)$ is the probability weighted Laplacian. Functional analytic considerations require introduction of the function spaces: $L^2(\rho)$ is the space of square integrable functions with respect to ρ with inner product $\langle f, g \rangle_{L^2} = \int f(x)g(x)\rho(x) \, dx$; $H^1(\rho)$ is the Hilbert space of functions in $L^2(\rho)$ whose first derivative, defined in the weak sense, is also in $L^2(\rho)$; and $H_0^1(\rho) = \{\psi \in H^1(\rho) \mid \int \psi(x)\rho(x) \, dx = 0\}$.

These definitions are important because $H_0^1(\rho)$ is the natural space for the solution ϕ of the Poisson equation (11). The operator $-\Delta_\rho$ is symmetric (self-adjoint) and positive definite because

$$-\langle f, \Delta_\rho g \rangle_{L^2} = \langle \nabla f, \nabla g \rangle_{L^2} = -\langle \Delta_\rho f, g \rangle_{L^2}, \quad \forall f, g \in H_0^1(\rho).$$

One requires an additional technical condition – the so-called Poincaré inequality – to conclude that the operator is in fact strictly positive-definite. Assuming the Poincaré inequality holds, it is also readily shown that Δ_ρ^{-1} is well defined, i.e., a unique solution $\phi \in H_0^1(\rho)$ exists for a given $h \in L^2(\rho)$ [44, Thm. 2].

For the purposes of numerical approximation, entirely analogous to the finite-dimensional case, the following equivalent formulations of the Poisson equation are introduced:

- 1) ϕ is a solution of the weak form

$$\langle \nabla \psi, \nabla \phi \rangle_{L^2} = \langle \psi, h - \hat{h} \rangle_{L^2} \quad \forall \psi \in H_0^1(\rho). \quad (\text{S14})$$

- 2) ϕ is a solution of the fixed-point equation

$$\phi = e^{t\Delta_\rho} \phi + \int_0^t e^{s\Delta_\rho} (h - \hat{h}) \, ds.$$

- 3) ϕ is the solution of the optimization problem

$$\min_{\phi \in H_0^1(\rho)} \frac{1}{2} \langle \nabla \phi, \nabla \phi \rangle_{L^2} + \langle \phi, h - \hat{h} \rangle_{L^2}. \quad (\text{S15})$$

These formulations have been used to develop numerical algorithms for gain function approximation:

- 1) Instead of $\psi \in H_0^1(\rho)$ in the weak form (S14), a relaxation is considered whereby $\psi \in S = \text{span}\{\psi_1, \dots, \psi_M\}$, a finite-dimensional subspace of $H_0^1(\rho)$. The resulting algorithm is referred to as the Galerkin algorithm for gain function approximation [44]. The constant gain formula (14) is obtained by considering S to be the subspace spanned by the coordinate functions.
- 2) The semigroup $e^{t\Delta_\rho}$ is approximated with the diffusion map operator T_ϵ as described in the main body of the paper. This approximation yields the diffusion map-based algorithm for gain function approximation, tabulated in the sidebar.
- 3) The optimization formulation (S15) is useful to explore nonlinear parametrizations of the gain function, e.g., using neural networks. A preliminary investigation of this appears in our paper [64]. Related deep learning-inspired techniques for solving PDEs using neural networks appear in [65].

Diffusion-map based algorithm for gain function approximation

Input: $\{X^i : 1 \leq i \leq N\}$, $\{h(X^i) : 1 \leq i \leq N\}$, kernel bandwidth ϵ

Output: $\{K^i : 1 \leq i \leq N\}$

- 1) $g_{ij} := e^{-\frac{|X^i - X^j|^2}{4\epsilon}}$ for $i, j = 1$ to N
- 2) $k_{ij} := \frac{g_{ij}}{\sqrt{\sum_l g_{il}} \sqrt{\sum_l g_{jl}}}$ for $i, j = 1$ to N
- 3) $d_i = \sum_j k_{ij}$ for $i = 1$ to N
- 4) $T_{ij} := \frac{k_{ij}}{d_i}$ for $i, j = 1$ to N
- 5) $\pi_i = \frac{d_i}{\sum_j d_j}$ for $i = 1$ to N
- 6) $\hat{h} = \sum_{i=1}^N \pi_i h(X^i)$
- 7) $\Phi = (0, \dots, 0) \in \mathbb{R}^N$
- 8) Solve the fixed point problem $\Phi = T\Phi + \epsilon(h - \hat{h})$ iteratively
- 9) $r_i = \Phi_i + \epsilon h_i$ for $i = 1$ to N
- 10) $s_{ij} = \frac{1}{2\epsilon} T_{ij} (r_j - \sum_{k=1}^N T_{ik} r_k)$ for $i, j = 1$ to N
- 11) $K^i = \sum_j s_{ij} X^j$ for $i = 1$ to N

Example: FPF for SIR models

The basic mathematical model of epidemiological disease propagation is the SIR ODE model:

$$\begin{aligned}\dot{S}_t &= -\beta S_t I_t, \\ \dot{I}_t &= \beta S_t I_t - \alpha I_t, \\ \dot{R}_t &= \alpha I_t,\end{aligned}$$

where S_t , I_t and R_t are the susceptible, infected and recovered population fractions, respectively, at time t . The parameters β and α are the transmission rate and the recovery rate parameters, respectively. In an epidemic, one observes the number of newly infected over a time-increment (daily). For our study, this is modeled as

$$dZ_t = (\beta I_t S_t) dt + \sigma_W dW_t, \quad (\text{S16})$$

where $W = \{W_t : t \geq 0\}$ is the standard w.p. and σ_W is the standard deviation (std. dev.) parameter. Given the observations, the filtering objective is to estimate the population sizes and possibly also the model parameters. In this study, the recovery rate parameter α is assumed known while the transmission rate parameter β is estimated. In a filtering setup, this requires a model which is assumed to be of the following form:

$$d\beta_t = \sigma_B dB_t,$$

where $B = \{B_t : t \geq 0\}$ is a standard w.p. and σ_B is the standard deviation parameter.

The model and the filter are simulated using the Euler discretization scheme for time integration. The simulation parameters are as follows: time discretization step-size $\Delta t = 1$; std. dev. for the observation noise $\sigma_W = 0.1$; std. dev. for the process noise $\sigma_B = 0.1$; initial distribution $I(0) \sim \text{unif}[0, 0.1]$ and $S(0) = 1 - I(0)$; recovery rate $\alpha = 0.1$; the transmission rate β is fixed to be 0.1 but assumed unknown to the filtering algorithm. The FPF is simulated using $N = 100$ particles. Two gain function approximation algorithms are implemented: the constant gain approximation and the diffusion map approximation. For the diffusion map approximation, the heuristic $\epsilon = 10 \text{med}(\{|X^i - X^j|^2; 1 \leq i, j \leq N\}) (\log(N))^{-1}$ is used, where $\text{med}(\cdot)$ denotes the statistical median. The simulation parameters and their values are tabulated in Table S1.

Figure S2 depicts the numerical results for the synthetic observation data generated using the model. Although the results depicted in the figure are illustrative as an application of FPF to the SIR models, additional work is necessary for its use in prediction with real COVID-19 data. This is because of the following reasons:

- 1) The observation model (S16) is not accurate. In the real-world settings, one only observes a certain unknown (and possibly time-varying and delayed) fraction of the newly infected population. This leads to fundamental issues with the identifiability of the transmission rate parameter β [66], [67]. Accurate estimation of β (or the closely associated non-dimensional reproduction number R_0) is important to capture the initial growth of the epidemic [68].
- 2) The 3-state SIR dynamic model is rather simplistic. This is because of several reasons: (i) The model assumes homogeneous well-mixed population while in practice there is strong evidence of heterogeneities [69] as well as spatial network effects [70]; (ii) The model is based on the underlying assumption of Markovian transitions between the epidemiological states. This assumption is contradicted by the experimental data on delay distributions [71]; and (iii) Even in the simplistic settings of the SIR model, the transmission rate parameter β is strongly time-varying. It is affected both by the individual choices (e.g., mask wearing) of the large number of agents as well as population-level government mandates (e.g., lockdown).

These difficulties notwithstanding, EnKF-based solutions to the COVID-19 data assimilation problem appear in [72], [73]. However, much work remains to be done on this important problem of immense societal importance. In the post-COVID reality, it is not inconceivable that surveillance and monitoring of infectious diseases such as seasonal flu will be as pervasive and common place as the weather tracking is today.

TABLE S1: Simulation parameters for the application of feedback particle filter to the epidemiological example.

parameter	notation	value
time step-size	Δt	1.0
observation noise	σ_W	0.1
process noise	σ_B	0.1
number of particles	N	100
recovery rate	α	0.1
transmission rate	β	0.1

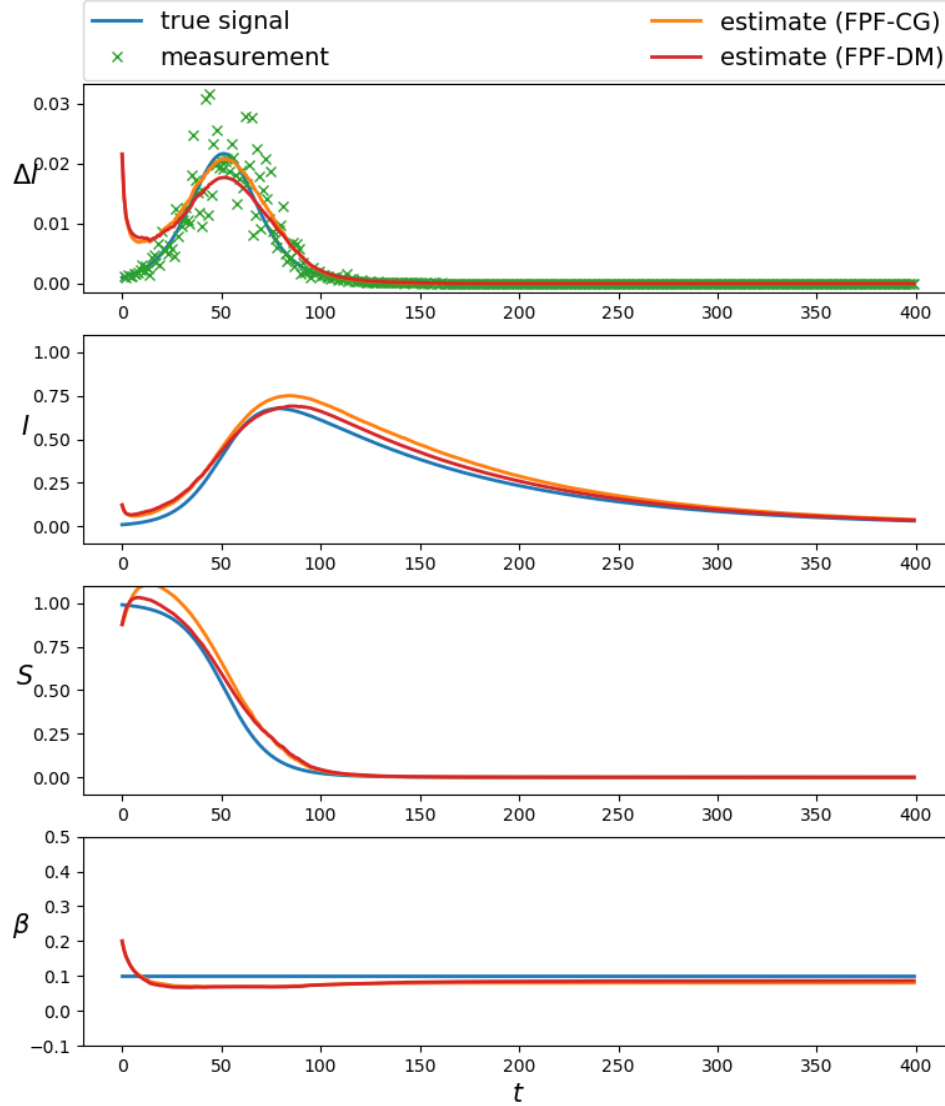


Figure S2: Application of the feedback particle filter on the SIR epidemiological model. The observation is the number of new confirmed cases each day ΔI (depicted in the top figure). The size of infected population is $I(t)$ and the size of susceptible population is $S(t)$. The infection transmission rate β is assumed unknown and it is estimated. The estimation algorithm is feedback particle filter with constant gain approximation (FPF-CG) and feedback particle filter with the diffusion map approximation (FPF-DM).